OPEN

Citation: Transl Psychiatry (2014) 4, e464; doi:10.1038/tp.2014.90

www.nature.com/tp

ORIGINAL ARTICLE

SLC6A3 coding variant Ala559Val found in two autism probands alters dopamine transporter function and trafficking

E Bowton[1,2,8], C Saunders[2,3,8], IA Reddy[1,2], NG Campbell[1,2], PJ Hamilton[1,2], LK Henry[4], H Coon[5], D Sakrikar[2,3], JM Veenstra-VanderWeele[2,6], RD Blakely[2,3], J Sutcliffe[1,2,6], HJG Matthies[1,2,7,9], K Erreger[1,2,7,9] and A Galli[1,2,7,9]

Emerging evidence associates dysfunction in the dopamine (DA) transporter (DAT) with the pathophysiology of autism spectrum disorder (ASD). The human DAT (hDAT; *SLC6A3*) rare variant with an Ala to Val substitution at amino acid 559 (hDAT A559V) was previously reported in individuals with bipolar disorder or attention-deficit hyperactivity disorder (ADHD). We have demonstrated that this variant is hyper-phosphorylated at the amino (N)-terminal serine (Ser) residues and promotes an anomalous DA efflux phenotype. Here, we report the novel identification of hDAT A559V in two unrelated ASD subjects and provide the first mechanistic description of its impaired trafficking phenotype. DAT surface expression is dynamically regulated by DAT substrates including the psychostimulant amphetamine (AMPH), which causes hDAT trafficking away from the plasma membrane. The integrity of DAT trafficking directly impacts DA transport capacity and therefore dopaminergic neurotransmission. Here, we show that hDAT A559V is resistant to AMPH-induced cell surface redistribution. This unique trafficking phenotype is conferred by altered protein kinase C β (PKCβ) activity. Cells expressing hDAT A559V exhibit constitutively elevated PKCβ activity, inhibition of which restores the AMPH-induced hDAT A559V membrane redistribution. Mechanistically, we link the inability of hDAT A559V to traffic in response to AMPH to the phosphorylation of the five most distal DAT N-terminal Ser. Mutation of these N-terminal Ser to Ala restores AMPH-induced trafficking. Furthermore, hDAT A559V has a diminished ability to transport AMPH, and therefore lacks AMPH-induced DA efflux. Pharmacological inhibition of PKCβ or Ser to Ala substitution in the hDAT A559V background restores AMPH-induced DA efflux while promoting intracellular AMPH accumulation. Although hDAT A559V is a rare variant, it has been found in multiple probands with neuropsychiatric disorders associated with imbalances in DA neurotransmission, including ADHD, bipolar disorder, and now ASD. These findings provide valuable insight into a new cellular phenotype (altered hDAT trafficking) supporting dysregulated DA function in these disorders. They also provide a novel potential target (PKCβ) for therapeutic interventions in individuals with ASD.

Translational Psychiatry (2014) **4,** e464; doi:10.1038/tp.2014.90; published online 14 October 2014

INTRODUCTION

Genetic factors are firmly established as important components in the etiology of autism spectrum disorder (ASD).[1] Rare genetic variation of nucleotides in protein-coding DNA (single-nucleotide variants (SNV) or small insertion/deletion variants (INDELS)), as well as rare genomic copy number variants, are significant risk factors for ASD and other neuropsychiatric disorders.[2–8] Several groups have conducted whole-exome sequencing on ASD families, and collectively, these studies indicate that discrete coding variants contribute to the overall genetic risk for ASD.[3,9–11] A hallmark of recent discoveries in this regard is that risk variants exhibit variable expressivity and incomplete penetrance. Thus, genetic variants associated with ASD can also occur in subjects presenting other neuropsychiatric conditions including attention-deficit hyperactivity disorder (ADHD).[12] Although *de novo* mutations can implicate a given genetic locus, single-nucleotide variants within the same gene are inherited and reported as possibly deleterious.[13,14]

The neurotransmitter dopamine (DA) has an important role in the central nervous system by regulating a variety of functions, including motor activity, motivation, attention and reward.[15–17] Disrupted DA function has been associated with a number of neuropsychiatric conditions, including ASD.[18–22] Consistent with this, DA dysfunction has been shown to occur in subjects with ASD within DA brain regions involved in reward processing, including the ventral striatum.[23,24] For example, Abrams *et al.*[25] found a striking pattern of underconnectivity between the voice-selective left posterior bilateral superior temporal sulcus and critical nodes in the dopaminergic system including the ventral tegmental area (VTA) and the nucleus accumbens (NAc) on resting state fMRI. The degree of underconnectivity between voice-selective cortex and reward pathways predicted severity of communication deficits in ASD children.[25] Consistently, a study by Gordon *et al.*[26] demonstrated that genetic variation in the dopamine transporter (DAT) impacts cross-network connectivity that correlates with measures of impulsivity and inattention, two

[1]Departments of Molecular Physiology and Biophysics, Vanderbilt University Medical Center, Nashville, TN, USA; [2]Vanderbilt Brain Institute, Vanderbilt University Medical Center, Nashville, TN, USA; [3]Department of Pharmacology, Vanderbilt University Medical Center, Nashville, TN, USA; [4]Department of Basic Sciences, University of North Dakota, Grand Forks, ND, USA; [5]Department of Psychiatry, University of Utah, Salt Lake City, UT, USA; [6]Department of Psychiatry, Vanderbilt University Medical Center, Nashville, TN, USA and [7]N-PISA Neuroscience Program In Substance Abuse, Vanderbilt University Medical Center, Nashville, TN, USA. Correspondence: Dr HJG Matthies or Dr K Erreger, Departments of Molecular Physiology and Biophysics, Vanderbilt University Medical Center, 465 21st Avenue South, MRB3, Room 7124, Nashville, TN 37232, USA or Dr A Galli, Departments of Molecular Physiology and Biophysics, Vanderbilt University Medical Center, 465 21st Avenue South, MRB3, Room 7130A, Nashville, TN 37232, USA.
E-mail: heiner.matthies@vanderbilt.edu or kevin.erreger@vanderbilt.edu or aurelio.galli@vanderbilt.edu
[8]These two authors contributed equally to this work.
[9]These authors contributed equally to this work.
Received 2 December 2013; revised 11 August 2014; accepted 12 August 2014

features of both ASD and ADHD.[27] These data underscore the significance of determining the molecular mechanisms underlying impairments within the dopaminergic system associated with ASD and related disorders with the intent to further define the etiology of this devastating disease.

The DAT is a key regulator of DA homeostasis and neurotransmission.[28] DAT function and expression in dopaminergic nodes have been linked to reward.[29–31] Notably, in humans, functional polymorphisms in DAT have been associated with neuropsychiatric disorders.[1,32–34] Genetic variation in the human DAT (hDAT; *SLC6A3*) also alters both anticipation and reception of rewards as well as motivational responses to social-emotional cues.[35–37] Consistent with a possible role of dysregulated DAT function in ASD, we recently identified and characterized the first *de novo* mutation in the hDAT associated with ASD.[32] This *de novo* mutation, T356M, causes profound impairments in hDAT function as well as related behaviors, suggesting a connection between ASD and disrupted DAT function.

Here, we report a second ASD-identified, hDAT missense mutation (hDAT A559V). Notably, hDAT A559V has been previously reported in one female with bipolar disorder[38] and independently in two male siblings with ADHD.[33] Previously, we have described an altered transport function in hDAT A559V,[1,34,39] namely the ability of hDAT A559V to support anomalous DA efflux (ADE) under basal conditions. Furthermore, the psychostimulant amphetamine (AMPH), known to cause reverse transport of DA in hDAT, fails to support AMPH-evoked DA efflux in hDAT A559V.[1,39] Here, we present novel insights in hDAT A559V-substrate recognition, hDAT A559V trafficking defects, a novel association of hDAT A559V with signaling pathways linked to ASD, as well as a mechanistic framework for ADE. These results implicate altered DA homeostasis as a potential complication associated with ASD.

MATERIALS AND METHODS

DNA sequencing of ASD subjects

The samples in the ARRA Autism Sequencing Consortium study consisted of 869 subjects ('cases') and 869 non-ASD comparison subjects ('controls').[40] ASD cases were previously assessed using the Autism Diagnostic Interview-Revised[41] and the Autism Diagnostic Observation Schedule-Generic|.[42] All cases met criteria for autism on the ADI and either autism or ASD on the Autism Diagnostic Observation Schedule-Generic|. ASD cases belong to various collections within the NIMH Center for Collaborative Genomic Studies of Mental Disorders (NIMH Repository; http://nimhgenetics.org) maintained at the Rutgers University Cell and DNA Repository (RUCDR; http://rucdr.org). Non-ASD control samples consist of subjects pair-matched to cases by Eigen vector analysis of genotype data to be of similar ancestry. All subjects provided informed consent, and the research was approved by each institutional board. Exome capture, sequencing, data processing and variant calling were conducted as described previously.[9,43,44] A559V variants were validated and inheritance within the respective families determined by Sanger sequencing of proband and parents. Amplifying primers were designed using Primer3 (http://frodo.wi.mit.edu/) and subjected to a BLAST-Like Alignment Tool search to ensure no significant matches existed elsewhere in the genome. Ideal annealing temperature was determined, and polymerase chain reaction carried out containing 7.1 nmol of amplifying primers and 12 ng of DNA in a final volume of 20 µl. Sequence analysis was performed using Sequencher v5.0.1 (Gene Codes, Ann Arbor, MI, USA).

Cell culture

The pcDNA3 expression vectors containing hDAT, hDAT A559V or hDAT A559V S/A sequence were used as described previously.[1,45] cDNA was transiently transfected into human embryonic kidney cells (HEK293) and co-transfected with enhanced green fluorescence protein (EGFP). Fugene-6 (Roche Molecular Biochemicals, Indianapolis, IN, USA) in serum-free media was used to transfect cells using a 1:3 DNA:lipid ratio. Assays were conducted 24 h after transfection.

AMPH transport

HEK-293 cells were transiently transfected with DNA, either hDAT or hDAT A559V, or vector alone (pcDNA3). Cells were serum-starved for 1 h, then washed three times with Krebs-Ringer-HEPES buffer. The Krebs-Ringer-HEPES assay buffer consisted of 130 mM NaCl, 1.3 mM KCl, 2.2 mM $CaCl_2$, 1.2 mM $MgSO_4$, 1.2 mM KH_2PO_4, 10 mM HEPES, 10 mM D-glucose, 100 µM pargyline, 10 µM tropolone, 100 µM ascorbic acid, pH 7.4. Cells were then treated with 10 nM AMPH for 5 min, washed three times, and extracted with acidic organic solvent. AMPH was quantified by reversed-phase high-performance liquid chormatography (HPLC) using the Waters AccQ·Tag method which uses pre-column derivatized reagents that help separate and easily detect fluorescence adducts (Waters, Milford, MA, USA). HPLC determinations were performed by the VBI/VKC Neurochemistry Core Lab, supported by Vanderbilt Kennedy Center for Research on Human Development and the Vanderbilt Brain Institute at the Vanderbilt University.

Cell surface biotinylation and immunoblotting

Cell surface biotinylation experiments were performed as described previously.[46–48] HEK-293 cells were seeded in six-well plates (10^6 cells per well) and transfected as described above 24 h before the experiment. Following AMPH treatment, cells were then incubated with sulfo-NHS-S-S-biotin (Pierce Chemical Company, Rockford, IL, USA) to label surface-localized transporter, and the biotinylated material was prepared and immunoblotted as described previously.[49] For PKCβ inhibition before AMPH treatment, cells were incubated for 20 min with 300 nM of the PKCβ inhibitor, 3-(1-(3-Imidazol-1-ylpropyl)-1H-indol-3-yl)-4-anilino-1H-pyrrole-2,5-dione (Calbiochem, Millipore EMD, Billerica, MA, USA). For immunoblots, DAT antibody (Chemicon International, Millipore EMD, #MAB369) was used at 1:1000 dilution, phospho-PKCβII/δ antibody (Santa Cruz Biotechnologies, Santa Cruz, CA, USA, #sc-11760) was used at 1:100 and β-actin antibody (Sigma, St Louis, MO, USA, #A5441) was used at 1:5000.

PKCβII activation

PKCβII activity assays were performed as described[50] with few modifications. Cells were pretreated with PMA (phorbol-12-myristate-13-acetate, 100 nM) or vehicle for 20 min. Thereafter, cells were washed once with cold PBS and then scraped into PBS containing protease inhibitors. The cells were lysed with a 27 gauge needle, sonicated and then spun at 800 *g* for 2 min to remove nuclear debris. The supernatant was then further centrifuged at 17 000 *g* for 40 min at 4 °C to yield cytosol (supernatant) and membrane (pellet). Comparable amounts of protein were then separated by 10% SDS–PAGE and then underwent western blotting using an antibody directed against phospho-PKCβII/δ (Santa Cruz Biotechnologies).

Transient currents

Changes in the hDAT transient charge (Q) movement were used to evaluate hDAT cell surface expression as described previously.[51–55] Cells were washed twice before recording with the external solution containing: 130 mM NaCl, 10 mM HEPES, 34 mM dextrose, 1.5 mM $CaCl_2$, 0.5 mM $MgSO_4$ and 1.3 mM KH_2PO_4, pH 7.35. For whole-cell patch clamp, quartz pipettes with a resistance of 3–5 MΩ were pulled on a P-2000 puller (Sutter Instruments, Novato, CA, USA) and filled with the internal solution containing 130 mM KCl, 0.1 mM $CaCl_2$, 2 mM $MgCl_2$, 1.1 mM EGTA, 10 mM HEPES and 30 mM dextrose adjusted to pH 7.35. hDAT-mediated transient currents in response to a voltage step from − 20 to − 140 mV, was obtained by integrating the 'on' step of the DAT-specific component of the AMPH-induced current (defined by subtracting the nonspecific current in the presence of 10 µM cocaine).

Amperometry

Cells plated on poly-D-lysine coated 35 mm dishes were transfected as described above and recorded 24 h later. For nonclamped amperometric experiments, cells were actively loaded with 1 µM DA in Krebs-Ringer-HEPES assay buffer for 20 min at 37 °C. Cells were washed twice with external solution before recording. GFP positive cells were selected for analysis and a carbon fiber electrode (Dagan, Minneapolis, MN, USA) was juxtaposed to the plasma membrane and held at +700 mV to oxidize DA. Amperometric currents were recorded at 25 °C using an Axopatch 200B amplifier digitized at 1 kHz and filtered with a low-pass Bessel filter at 100 Hz. Data were filtered offline at 1 Hz before analysis. AMPH-induced DA

efflux was defined as the current recorded in the presence of 10 μM AMPH minus the baseline current recorded before the addition of AMPH. For amperometry using the PKCβII peptide inhibitor, 2 mM DA and 10 μM of the peptide (or scramble peptide) was added to pipette solution and cells were whole-cell patch clamped at −20 mV for 10 min. The patch electrode was then lifted off the cell, while the cell remained intact. Nonclamped amperometric data were then recorded using a carbon fiber electrode held at +700 mV.

RESULTS

Identification of SLC6A3 A559V in autism spectrum disorder subjects

The ARRA Autism Sequencing Consortium whole-exome sequencing data used in this study consisted of 869 previously described ASD subjects[9,43,44] and 869 non-ASD control subjects selected to be of similar ancestry. Exome capture and sequencing analysis identified two ASD samples harboring the *SLC6A3* A559V genotype. None were found in the control comparison samples. In both instances of an *SLC6A3* A559V variant (Chr5:14303128; hg19), validation was conducted using Sanger sequencing, followed by assessment of inheritance patterns in all available family members (Figure 1). Both ASD subjects harboring the *SLC6A3* A559V mutation are non-consanguineous males with normal IQ and no history of seizures or other related medical comorbidities (see Supplementary Data 1). Considering that dysregulated DA neurotransmission has been associated with ASD,[20–22,25,32] we next mechanistically determined whether hDAT A559V harbors functional defects that could impact proper DA homeostasis.

hDAT A559V has impaired AMPH transport

hDAT membrane expression is dynamically regulated by several signaling pathways.[56] Notably, this regulation is effectively impaired by the psychostimulant AMPH that causes a reduction in DAT expression at the plasma membrane.[49,53,57–59] A mechanistic feature of AMPH-like psychostimulants is the requirement for AMPH to be transported across the plasma membrane to induce pharmacological actions including hDAT trafficking.[60,61] We have previously shown that in hDAT A559V cells, AMPH fails to induce reverse transport of DA.[1,45] This suggests the possibility that hDAT A559V has reduced ability to transport AMPH. Therefore, to begin elucidating functional distinctions between hDAT A559V and hDAT, we explored hDAT A559V-mediated AMPH transport. This is clinically relevant as racemic AMPH (Adderall) is effectively used for treating ADHD symptoms in ASD individuals.[22,62,63]

AMPH transport was quantified by HPLC in hDAT and hDAT A559V cells (HEK-293T transiently expressing either hDAT or hDAT A559V). AMPH transport was performed at a concentration of 10 nM AMPH to avoid nonspecific AMPH plasma membrane accumulation occurring at higher AMPH concentrations.[60,64] AMPH is lipophilic resulting in nonspecific membrane incorporation in a time and temperature independent way, interfering with resolving AMPH transport at micromolar concentrations.[64] Following exposure to 10 nM AMPH, hDAT cells accumulate ~3 times the amount of AMPH compared with empty vector control cells (Figure 2a, compare solid bar 'hDAT' with striped bar 'pcDNA3'). AMPH transport by hDAT is blocked by pretreatment with 10 μM cocaine ('hDAT+cocaine'). However, cells expressing hDAT A559V do not accumulate AMPH to a greater degree than empty vector control cells (Figure 2a, compare open bar 'hDAT A559V' with striped bar 'pcDNA3'). The inset demonstrates that hDAT and hDAT A559V have comparable DAT expression levels, as previously shown.[1,45] Therefore, AMPH, although capable of binding to hDAT A559V and modifying its function,[1,45] is not an efficiently transported substrate. As expected, due to nonspecific membrane incorporation, no significant difference was observed between hDAT, hDAT A559V and empty vector transfected cells using 10 μM AMPH ($n=6$; $P \geqslant 0.05$).

To circumvent nonspecific membrane incorporation at 10 μM AMPH, AMPH-induced whole-cell inward currents were measured in a real time functional assay in response to AMPH rapid application. AMPH binds to hDAT and induces an inward electrical current that is proportional to substrate transport.[65] Therefore, the substrate (AMPH)-induced inward current is an indirect index of substrate transport. Cells expressing either hDAT or hDAT A559V were whole-cell voltage clamped at −20 mV (the typical membrane potential of our cell line) and AMPH (10 μM) was bath applied. Compared with hDAT cells, hDAT A559V cells exhibited a significantly lower amplitude current response to 10 μM AMPH (hDAT A559V 63 ± 18% of hDAT, $P < 0.05$, Student's *t*-test, $n=3$). This result demonstrates that AMPH-induced whole-cell current is reduced in hDAT A559V, reflecting a decrease in AMPH

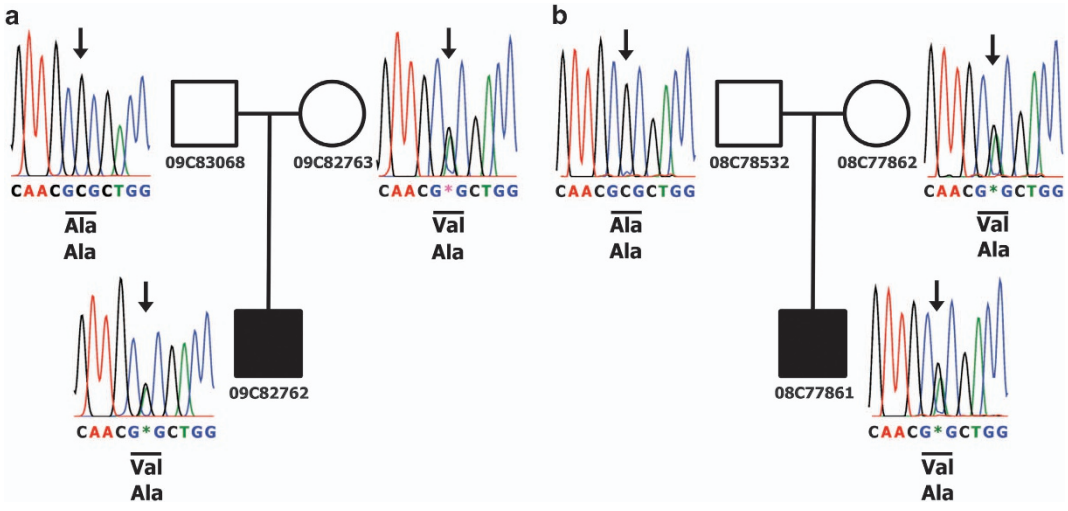

Figure 1. Validation of the hDAT A559V variant in two unrelated ASD probands. (**a** and **b**) Sanger sequence validation is shown for the two proband cases of the A559V genotype in the study. Chromatogram data is shown with the corresponding coding sequence flanking amino acid residue 559. Variant-nucleotide sequence is indicated by an asterisk representing heterozygous C/T at this position. Filled symbols indicate individuals with an ASD diagnosis, whereas open symbols reflect individuals without an ASD diagnosis. The circles represent females and the squares males. Individual IDs in the respective pedigrees correspond to NIMH cell line IDs. ASD, autism spectrum disorder.

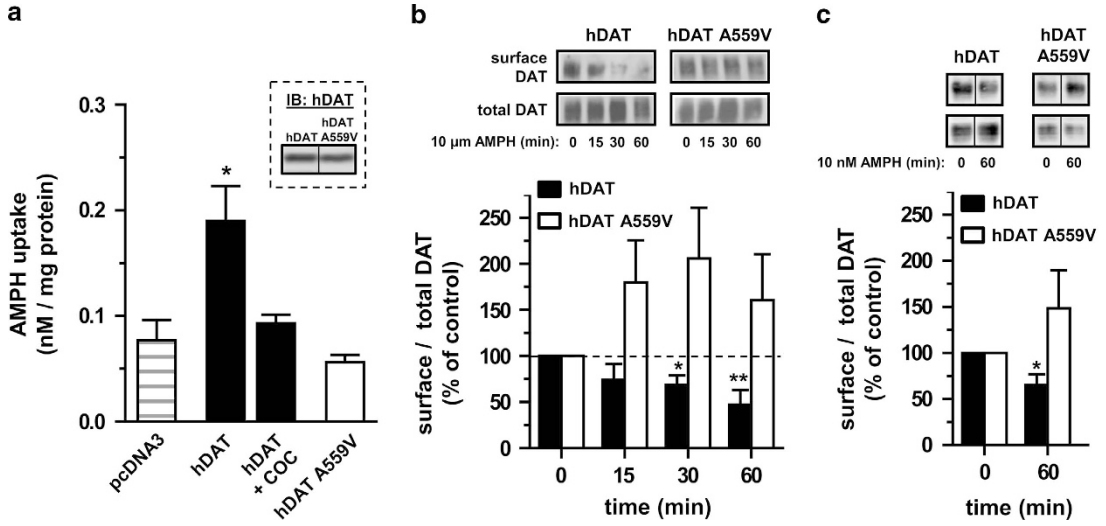

Figure 2. hDAT A559V does not transport AMPH. (**a**) Uptake was performed with 10 nM AMPH for 5 min in cells transfected with either empty vector (pcDNA3), hDAT or hDAT A559V. hDAT cells exhibited robust AMPH uptake blocked by pretreatment with 10 µM cocaine (*$P < 0.05$, one-way analysis of variance (ANOVA) followed by Dunnett's multiple comparison test, $n = 3$). hDAT A559V cells exhibited uptake not significantly different from the empty vector control ($P > 0.05$, one-way ANOVA followed by Dunnett's multiple comparison test, $n = 3$). *inset:* representative immunoblot for DAT demonstrates comparable levels of transporter expression between hDAT and hDAT A559V cells. (**b**) hDAT or hDAT A559V cells were treated with AMPH (10 µM) for the indicated time points. Top, representative immunoblot of DAT biotinylated proteins ('surface DAT') and total cellular lysate ('total DAT') following AMPH (10 µM) treatment. Bottom, quantification of biotinylated DAT protein fractions following AMPH treatment. The ratio of surface to total DAT protein is plotted normalized to time point 0 (no AMPH treatment). AMPH decreases surface DAT in hDAT cells, but not in hDAT A559V cells (**$P < 0.01$, *$P < 0.05$, one-way ANOVA followed by Dunnett's multiple comparison test, $n = 6$). (**c**) hDAT or hDAT A559V cells were treated with AMPH (10 nM) for the indicated time points. Top, representative immunoblot of DAT biotinylated fraction ('surface DAT') and total cellular lysate ('total DAT'). Bottom, quantification of biotinylated DAT protein fractions following AMPH treatment. The ratio of surface to total DAT protein is plotted normalized to time point 0 (no AMPH treatment). The 10 nM concentration of AMPH decreases surface DAT in hDAT cells, but not in hDAT A559V cells (*$P < 0.05$, Student's *t*-test, $n = 4$). AMPH, amphetamine; DAT, dopamine transporter; hDAT, human dopamine transporter.

accumulation at a concentration of 10 µM and further supporting our results obtained by HPLC at a lower AMPH concentration.

An important action of AMPH is to reduce DAT surface levels.[49,61] Both actions are thought to be dependent on intracellular accumulation of AMPH through its transport by DAT.[60,61] In hDAT A559V cells, AMPH transport into the cell is impaired (Figure 2a). Therefore, we next examined whether the A559V variant affects AMPH-induced DAT cell surface redistribution. We measured cell surface expression of DAT in either hDAT or hDAT A559V cells exposed to AMPH (10 µM) for different time periods by means of biotinylation. Representative DAT immunoblots for hDAT and hDAT A559V cells are displayed (Figure 2b, top) for both the biotinylated ('surface DAT') fraction and total cell lysates ('total DAT'). The graph quantifies the ratio of surface to total DAT, normalized to the control condition (time 0) for hDAT and hDAT A559V cells (Figure 2b, bottom). AMPH treatment induces a significant loss of cell surface DAT in hDAT cells (Figure 2b, solid bars, bottom), consistent with previous reports.[49,53,57–59] Notably, AMPH fails to induce DAT cell surface loss in hDAT A559V cells (Figure 2b, open bars, bottom), putatively due to a lack of intracellular AMPH accumulation.

Importantly, the 10 nM concentration of AMPH used for the assay is sufficient to cause both significant hDAT cell surface redistribution, as measured by immunoblotting of biotinylated fractions (Figure 2c, compare solid bar 'hDAT' vs open bar hDAT A559V') as well as DA efflux (0.25 ± 0.04 pA; $P < 0.05$ by Student's *t*-test with respect to baseline; $n = 4$). These data demonstrate that 10 nM AMPH is a functionally relevant concentration and further strengthen our conclusion that hDAT A559V has diminished AMPH transport.

Intracellular, but not extracellular, AMPH delivery induces hDAT A559V trafficking

To measure changes in DAT surface expression induced by AMPH, we also utilized the established electrophysiological method of measuring DAT-mediated transient currents.[51–55] In response to a hyperpolarizing voltage jump, DAT-expressing cells display current relaxations (transient currents) that persist after the time required for charging the capacitance of the cell membrane. The DAT-specific component of these current relaxations (DAT-mediated transient current) is defined by subtracting the nonspecific current recorded in the presence of the DAT inhibitor cocaine. The transient currents originate from charge movement in each single DAT promoted by the voltage jump. The integral of the DAT-specific transient current is the DAT-mediated transient charge movement (Q) that is proportional to DAT cell surface expression.[51–55] In particular, AMPH induces a time-dependent decrease in Q that temporally correlates with AMPH-induced DAT trafficking as measured by cell surface biotinylation, quasi stationary noise analysis and confocal imaging.[53,54] Figure 3 shows transient currents elicited by stepping the membrane voltage from −20 to −140 mV. This voltage is saturating for the magnitude of DAT-mediated transient currents and transient currents at this voltage are not altered by the presence of DAT substrates.[53] DAT-mediated transient currents from both hDAT and hDAT A559V cells under control conditions before AMPH treatment (control) are displayed as dotted lines (Figure 3a, top). Following AMPH treatment (10 µM for 10 min), the transient current is reduced in hDAT cells (Figure 3a, top, compare AMPH solid line to control dotted line), indicating that AMPH induces a redistribution of DAT away from the plasma membrane. However, for hDAT A559V cells, AMPH does not reduce the transient current (Figure 3a, top, compare AMPH solid line to control dotted line). The DAT-mediated transient charge movement (Q) in response to

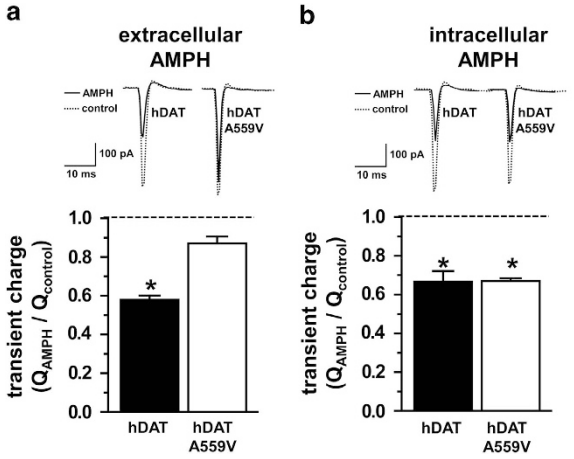

Figure 3. Intracellular AMPH delivery induces trafficking in hDAT A559V cells measured by transient charge movement. (**a**) Cells were voltage clamped in the whole-cell configuration at a baseline of − 20 mV and the current recorded following a voltage step to − 140 mV. DAT-mediated currents were defined by subtracting the nonspecific current obtained in the presence of the DAT blocker cocaine (10 μM) from those recorded in the absence of cocaine. Top, DAT-mediated control currents (dotted lines) before AMPH treatment are plotted and compared with currents recorded after AMPH treatment (10 μM AMPH for 10 min, solid lines). Extracellular AMPH induces DAT trafficking (compare AMPH solid lines with control dotted lines) in hDAT but not hDAT A559V cells. Bottom, the transient charge (Q) was obtained by integrating the area under transient current as an index of the number of transporters at the cell surface. AMPH significantly decreases Q in hDAT cells (*$P < 0.05$, Q_{AMPH} vs $Q_{control}$ Student's *t*-test, $n = 5$) but not hDAT A559V cells ($P > 0.05$, Q_{AMPH} vs $Q_{control}$ Student's *t*-test, $n = 3$). (**b**) AMPH was applied intracellularly through perfusion by the whole-cell patch clamp pipette internal solution. Top, DAT-mediated control currents immediately after achieving whole-cell access (dotted lines) are plotted compared with currents after perfusing the cell for 10 min with AMPH (10 μM, solid lines). AMPH does induce DAT trafficking of hDAT A559V cells comparable to that of hDAT cells. Bottom, AMPH significantly decreases Q in both hDAT and hDAT A559V cells (*$P < 0.05$, Q_{AMPH} vs $Q_{control}$ Student's *t*-test, $n = 3$). AMPH, amphetamine; DAT, dopamine transporter; hDAT, human dopamine transporter.

the voltage jump was quantified by integrating the DAT-mediated transient current for both hDAT and hDAT A559V cells and normalized to respective controls (Figure 3a, bottom). This DAT-mediated charge movement Q is proportional to plasma membrane levels of DAT.[51–55] Extracellular bath application of AMPH significantly decreases Q for hDAT cells but not for hDAT A559V cells (Figure 3a, bottom). These results corroborate the biochemical data demonstrating that hDAT A559V cells are resistant to AMPH-induced trafficking (Figure 2b).

Intracellular AMPH accumulation is required for AMPH to cause DAT redistribution away from the plasma membrane.[61] Figure 2a demonstrates that hDAT A559V is impaired in AMPH accumulation. Thus, we next determined whether the resistance of hDAT A559V to trafficking upon AMPH exposure stems from its reduced ability to transport AMPH. While recording DAT-mediated transient currents to monitor changes in plasma membrane levels of DAT, we used the whole-cell patch clamp pipette to directly deliver intracellular AMPH to hDAT and hDAT A559V cells. This methodology bypasses DAT function to induce intracellular accumulation of AMPH. Immediately after breaking through the membrane to achieve whole-cell access of the patch clamp pipette, control transient currents from both hDAT and hDAT A559V cells were recorded (Figure 3b, top, dotted lines). In this experiment, AMPH (10 μM) was added to the patch pipette internal solution and allowed to dialyze the cytoplasm of the cell. Following 10 min of intracellular delivery of AMPH, transient currents from both hDAT and hDAT A559V cells were recorded (Figure 3b, top, solid lines). For both hDAT and hDAT A559V cells, intracellular AMPH reduced the magnitude of transient currents (Figure 3b, top, compare control dotted line to AMPH solid line). The quantification of DAT-mediated transient charge movement (Q) for the AMPH condition normalized to the respective control condition (transient current recorded after breaking through the membrane) is shown for both hDAT and hDAT A559V (Figure 3b, bottom). Intracellular AMPH application decreases Q for both hDAT cells and for hDAT A559V cells (Figure 3b, bottom). Thus, intracellular perfusion of AMPH, which bypasses the requirement of DAT uptake function to accumulate intracellularly, restores the ability of AMPH to cause hDAT A559V trafficking. These data suggest that hDAT A559V cells retain the machinery necessary for AMPH to induce trafficking, but the impairment in AMPH accumulation prevents DAT redistribution away from the plasma membrane in response to AMPH.

PKCβ inhibition restores AMPH-induced hDAT A559V cell surface redistribution

DAT surface expression is tightly regulated by several signaling pathways and receptors, including DA D2 receptors (D2R).[28,47,48,54,66–73] We have shown that hDAT A559V-mediated ADE involves D2R activation and that D2Rs are endogenously expressed and tonically active in hDAT A559V cells.[1] D2Rs act through multiple signaling pathways including PKCβ. Notably, D2R activation regulates DAT surface expression in a PKCβ-dependent manner.[66] Therefore, one possibility is that hDAT A559V resistance to AMPH-induced cell surface redistribution is due to elevated basal PKCβ activity. PKCβII is an alternatively spliced isoform of PKCβI that has been shown to interact with DAT and to promote DA efflux.[74] PKC translocation to the plasma membrane has classically been considered the hallmark of activation. However, there is some evidence that PKCβII activation is a more complex process not exclusively determined by translocation to the plasma membrane.[75] Therefore, we used autophosphorylation of PKCβII at Ser660 as a readout of PKCβII function.[76,77] We next examined whether constitutive levels of phospho-PKCβII are altered in cells expressing hDAT A559V both at the plasma membrane and in the cytosol.

Figure 4a shows that basal levels of phospho-PKCβII in the cytosolic fraction of hDAT A559V cells are comparable to those of hDAT cells (Figure 4a, 'cytosol'). However, phospho-PKCβII is significantly elevated in the membrane fraction of hDAT A559V cells compared with hDAT cells (Figure 4a, 'membrane'). The membrane protein Na/K ATPase is shown as a loading control (Figure 4a, Na/K ATPase). Quantification of immunoblots for membrane fraction basal phospho-PKCβII is shown in the bar graph (Figure 4a, bottom), normalized to Na/K ATPase for each sample and expressed as a percentage of hDAT. PMA (100 nM, 20 min.) was used as a positive control to show activation of PKCβII in hDAT cells. PMA significantly increases phospho-PKCβII (268 ± 70% of basal hDAT, $n = 3$, $P < 0.05$, ANOVA followed by Newman–Keuls multiple comparison test) in the membrane fraction in hDAT cells to a level not significantly different from basal phospho-PKCβII in A559V cells ($P > 0.05$, ANOVA followed by Newman–Keuls multiple comparison test). These data show that phospho-PKCβII is constitutively elevated at the plasma membrane in hDAT A559V cells and suggest a possible role for PKCβ activity in the trafficking deficits of hDAT A559V.

Therefore, we next examined whether the inability of hDAT A559V to traffic upon AMPH exposure depends on increased PKCβ activity. hDAT A559V cells were pretreated with a PKCβ inhibitor, (3-(1-(3-Imidazol-1-ylpropyl)-1H-indol-3-yl)-4-anilino-1H-pyrrole-2,5-dione; 300 nM for 20 min), and then with either AMPH (10 μM

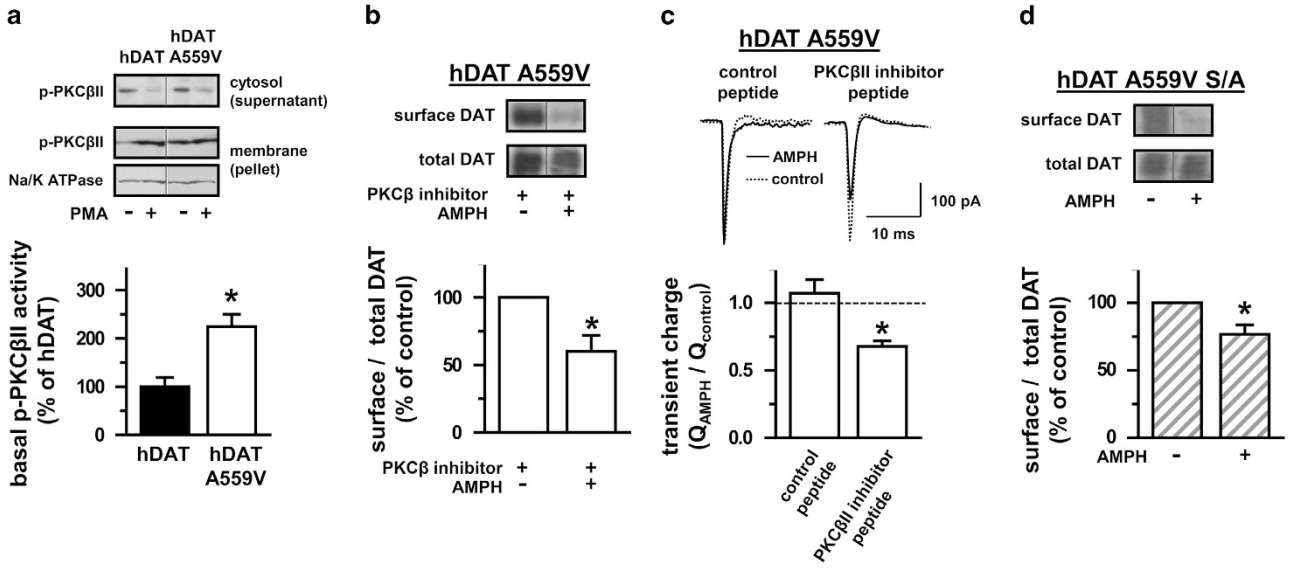

Figure 4. PKCβ inhibition restores AMPH-induced hDAT A559V internalization. (**a**) Representative immunoblots of phospho-PKCβII in hDAT and hDAT A559V cells. The top bands represent PKCβ in the cytosolic fraction. The middle bands represent PKCβ in the membrane fraction. PMA (100 nM for 20 min) was used as a positive control to demonstrate phosphorylation and translocation of PKCβ to the membrane in hDAT cells. The membrane protein Na/K ATPase (bottom bands) is used as a loading control for the membrane fraction. The bar graph shows that basal levels of phospho-PKCβII in the membrane fraction are higher in hDAT A559V cells than hDAT cells (*$P < 0.05$, Student's *t*-test, $n = 6$–8). (**b**) Cells were treated for 20 min with the PKCβ inhibitor 3-(1-(3-Imidazol-1-ylpropyl)-1H-indol-3-yl)-4-anilino-1H-pyrrole-2,5-dione (300 nM) before treatment with vehicle or AMPH (10 μM, 60 min). Top, representative immunoblot of DAT biotinylated proteins ('surface DAT') and total lysate ('total DAT'). Bottom, quantification of surface to total DAT ratio. PKCβ inhibition restores AMPH-induced trafficking of hDAT A559V (AMPH vs vehicle, *$P < 0.05$ Student's *t*-test, $n = 4$). (**c**) Transient currents were recorded as an index of surface DAT in hDAT A559V cells. Cells were dialyzed under whole-cell patch clamp for 10 min with internal solution containing either the PKCβII inhibitor peptide (N-Myr-SLNPEWNET, 10 μM) or a scramble peptide (10 μM). Top, subsequent DAT-mediated currents following a voltage step from − 20 mV to − 140 mV are plotted for control (dotted lines) compared with currents after extracellular AMPH treatment (10 μM AMPH for 10 min, solid lines). PKCβII inhibition restores the AMPH-induced decrease in transient current in hDAT A559V cells. Bottom, AMPH decreases transient charge movement Q in hDAT A559V cells treated with PKCβII inhibitor peptide (*$P < 0.05$, Q_{AMPH} vs $Q_{control}$ Student's *t*-test, $n = 4$) but not scramble peptide ($P > 0.05$, Q_{AMPH} vs $Q_{control}$ Student's *t*-test, $n = 4$). (**d**) hDAT A559V S/A cells were treated with vehicle or AMPH (10 μM, 60 min). Top, representative immunoblot of DAT biotinylated proteins ('surface DAT') and total cellular lysate ('total DAT'). Bottom, quantification of surface to total DAT ratio. Mutation of N-terminal Ser to Ala in hDAT A559V restores AMPH-induced trafficking (AMPH vs vehicle, *$P < 0.05$ Student's *t*-test, $n = 4$). AMPH, amphetamine; DAT, dopamine transporter; hDAT, human dopamine transporter.

AMPH for 60 min) or vehicle control. Remarkably, inhibition of PKCβ restores AMPH-induced trafficking of hDAT A559V as determined by cell surface biotinylation (Figure 4b, top). Quantification of multiple experiments is shown in Figure 4b (bottom). In contrast, AMPH-induced DAT trafficking in wild-type hDAT cells is not significantly different in the presence vs absence of the PKCβ inhibitor (PKCβ inhibitor vs vehicle; $P > 0.05$, Student's *t*-test, $n = 3$–6). Therefore, PKCβ inhibition restores AMPH-induced DAT trafficking in hDAT A559V cells, but has no effect on AMPH-induced DAT trafficking in hDAT cells. These data suggest that PKCβ regulation of AMPH-induced cell surface redistribution may be more relevant in DA systems altered by genetic variants such as hDAT A559V than under typical physiological signaling environments.

To further confirm that PKCβ inhibition restores AMPH actions through PKCβII-dependent intracellular signaling, we measured DAT-mediated transient currents as an index of AMPH-induced changes in DAT cell surface expression following PKCβ inhibition by a PKCβII inhibitor peptide (N-myr-SLNPEWNET)[78] delivered intracellularly through the patch clamp pipette. Transient currents were elicited from hDAT A559V cells by stepping the membrane voltage from − 20 to − 140 mV as in Figure 3. Figure 4c shows representative DAT-mediated transient currents recorded from hDAT A559V cells following intracellular perfusion for 10 min with either the PKCβII inhibitor peptide (N-myr-SLNPEWNET; 10 μM) or a scramble peptide (N-myr-ETWENPSNL, 10 μM). Transient currents before AMPH application (control) are displayed as dotted lines and transient currents following AMPH extracellular bath application (10 μM for 10 min) are displayed as solid lines (Figure 4c, top). In hDAT A559V cells perfused with the scramble peptide, AMPH does not alter the transient current indicating the absence of AMPH-induced trafficking (Figure 4c, top, scramble peptide). In hDAT A559V cells perfused with the PKCβII inhibitor peptide, AMPH decreases the transient current indicating the restoration of DAT trafficking by PKCβ inhibition (Figure 4c, top, PKCβII inhibitor peptide). The total transient charge movement Q in response to the voltage jump was quantified by integrating the DAT-specific transient currents as an index of DAT surface levels (Figure 4c, bottom). Consistent with biochemical measurements of DAT trafficking by biotinylation with a small molecule PKCβ inhibitor (Figure 4b), PKCβ inhibition with a peptide inhibitor restores AMPH-induced hDAT A559V trafficking as indicated by the reduction in transient currents recorded electrophysiologically. Intracellular accumulation of AMPH is required for AMPH-induced trafficking therefore we next confirmed that PKCβ inhibition increases AMPH accumulation by hDAT A559V. AMPH transport was quantified by HPLC with a concentration of 10 nM AMPH as in Figure 2a. hDAT A559V cells were pretreated with a PKCβ inhibitor (3-(1-(3-Imidazol-1-ylpropyl)-1H-indol-3-yl)-4-anilino-1H-pyrrole-2,5-dione; 300 nM for 20 min) or vehicle control. PKCβ inhibition increases AMPH accumulation by 73 ± 20% with respect to vehicle control ($P < 0.05$, Student's *t*-test, $n = 3$).

Previously, we reported increased DAT amino (N)-terminal phosphorylation at N-terminal serine (Ser) residues 7, 12 and 13 in hDAT A559V cells with respect to hDAT cells.[1] Indeed, hDAT A559V must be N-terminal phosphorylated to display ADE.[1] Thus,

we examined whether hDAT A559V must be N-terminal phosphorylated to impair AMPH-induced DAT cell surface redistribution. We used the hDAT A559V S/A construct (as described previously in Bowton *et al.*[1]), in which the five most distal N-terminal Ser are mutated to Ala in the hDAT A559V background to prevent phosphorylation of the DAT N terminus (hDAT A559V S/A). Figure 4d (top) shows that AMPH-induced DAT cell surface redistribution is restored in hDAT A559V S/A cells. Quantification of the surface to total DAT ratio is shown in Figure 4d (bottom). These data indicate that phosphorylation of the N terminus contributes to the inability of AMPH to induce trafficking of hDAT A559V.

In Figures 2 and 3, we demonstrate that the diminished hDAT A559V AMPH-induced trafficking stems from a reduced intracellular accumulation of AMPH. Therefore, it is possible that the restored ability of AMPH to cause hDAT A559V S/A trafficking (Figure 4d) is due to restored AMPH transport. Substrate-induced inward current is an indirect index of substrate transport and action at the DAT.[65] Cells expressing either hDAT or hDAT A559V S/A were whole-cell voltage clamped at −20 mV and AMPH (10 μM) was applied by bath perfusion. In contrast to hDAT A559V, hDAT A559V S/A AMPH-induced inward whole-cell currents are no different from that of hDAT (hDAT A559V S/A 110 ± 15% of hDAT, $P > 0.05$, Student's *t*-test, $n = 3$). These data further support the notion that Ser to Ala substitutions in the A559V background restores AMPH transport. To confirm this conclusion by an independent method, AMPH transport was quantified by HPLC with a concentration of 10 nM AMPH for hDAT A559V S/A cells compared with hDAT A559V cells. Ser to Ala mutations in the A559V background increased AMPH accumulation by 60 ± 10% (hDAT A559V S/A with respect to hDAT A559V; $P < 0.05$, Student's *t*-test, $n = 3$).

PKCβ inhibition restores AMPH-induced DA efflux in hDAT A559V

Previously, we reported ADE in hDAT A559V cells.[1,39] ADE stems from constitutive reverse transport of DA mediated by hDAT A559V. Notably, hDAT A559V-mediated ADE is inhibited by AMPH.[1,39] In the present study we demonstrate that hDAT A559V does not transport AMPH, and as a result, is rendered insensitive to the trafficking actions of AMPH. This is consistent with our previous observations that AMPH acts as an inhibitor of hDAT A559V to reduce ADE, rather than inducing DA efflux.[1,39] Figure 4 demonstrates that PKCβ as well as N-terminal phosphorylation mediate the inability of AMPH to cause hDAT A559V cell surface redistribution. Thus, we sought to determine whether PKCβ activity and DAT N-terminal phosphorylation have a role in ADE for hDAT A559V cells. We used amperometry to measure DA efflux by oxidation/reduction reactions[1,39] from cells transfected with either hDAT, hDAT A559V or hDAT A559V S/A. Positive amperometric currents represent DA efflux (DA leaving the cell). Cells were bath loaded with DA (1 μM) via DAT-mediated uptake and subsequent AMPH-induced DA efflux was measured by amperometry.[1,39] hDAT A559V cells have normal uptake of DA that is not significantly different from hDAT cells.[1,34,45] Cocaine (10 μM) was used here to demonstrate DAT specificity of the amperometric signal. Amperometric current traces in response to 10 μM AMPH in hDAT cells are displayed in Figure 5a (top). AMPH-induced DA efflux is defined as the efflux induced by AMPH with respect to the baseline (before AMPH application) and quantification of multiple experiments is shown in the bar graph (Figure 5a, bottom). We first examined the role of PKCβ on AMPH-induced DA efflux by pretreating hDAT cells with the PKCβ inhibitor 3-(1-(3-Imidazol-1-ylpropyl)-1H-indol-3-yl)-4-anilino-1H-pyrrole-2,5-dione and measuring AMPH-induced DA efflux. PKCβ inhibition has no significant effect on AMPH-induced hDAT-mediated DA efflux (Figure 5a, compare solid bars ± PKCβ inhibitor). In hDAT A559V cells, in the absence of the PKCβ inhibitor, AMPH blocks a

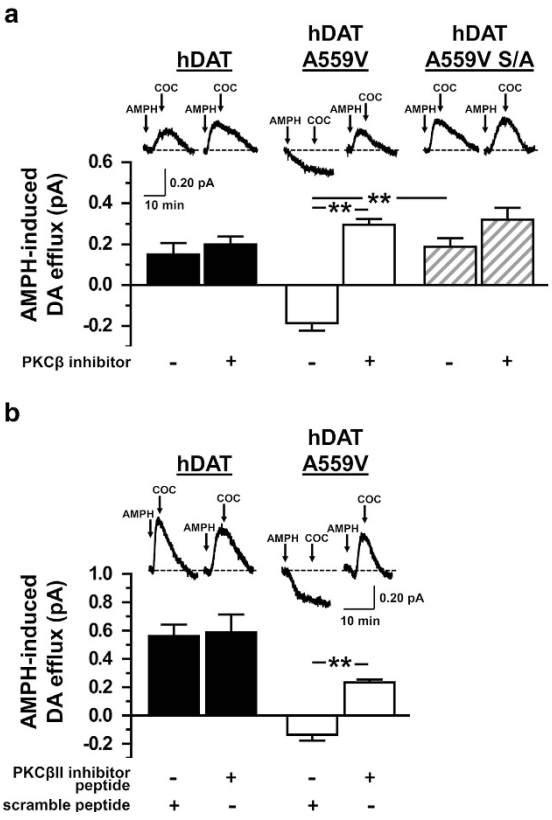

Figure 5. AMPH-induced DA efflux is impaired in hDAT A559V cells but restored by inhibiting PKCβ activity or mutating N-terminal Ser to Ala. (**a**) Representative amperometric traces (top) and quantification of amperometric DA signals (bottom) recorded in hDAT, hDAT A559V, and hDAT A559V S/A cells following 20 min pretreatment with either vehicle control or the PKCβ inhibitor 3-(1-(3-Imidazol-1-ylpropyl)-1H-indol-3-yl)-4-anilino-1H-pyrrole-2,5-dione (300 nM). Arrows indicate addition of AMPH (10 μM) or cocaine (COC, 10 μM) to the extracellular bath. AMPH increases amperometric currents from hDAT cells, indicating DA efflux. However, AMPH reduces amperometric currents in hDAT A559V cells, indicating a block of basal DA efflux from hDAT A559V cells. Either pretreatment with the PKCβ inhibitor or mutation of N-terminal serines in hDAT A559V restores the ability of AMPH to induce DA efflux in hDAT A559V cells (**$P < 0.01$ analysis of variance (ANOVA) followed by Newman–Keuls multiple comparison test, $n = 3$–5). (**b**) Cells were patch clamped and perfused through the whole-cell patch pipette for 10 min to allow for loading of 2 mM DA and either the PKCβ inhibitor peptide (N-Myr-SLNPEWNET, 10 μM) or a scramble control peptide (10 μM). The patch pipette was then withdrawn and AMPH-induced DA signals recorded by amperometry. The PKCβ inhibitor peptide restores the ability of AMPH to induce DA efflux in hDAT A559V cells (**$P < 0.01$ ANOVA followed by Newman–Keuls multiple comparison test, $n = 3$). AMPH, amphetamine; DA, dopamine; DAT, dopamine transporter; hDAT, human dopamine transporter.

constitutive ADE, reflected by a decrease in the amperometric current from baseline (Figure 5a, top). Importantly, PKCβ inhibition restores the ability of AMPH to cause DA efflux in hDAT A559V cells (Figure 5a, top). Figure 5a (bottom) shows quantification of multiple experiments (compare open bars ± PKCβ inhibitor). In light of our data showing elevated basal PKCβ activity in hDAT A559V cells (Figure 4a), it is possible that PKCβ, through phosphorylation of the hDAT A559V N terminus, is responsible for the inability of hDAT A559V to transport AMPH, thereby affecting both DAT trafficking and DA efflux. Notably, AMPH-induced DA efflux is restored in hDAT A559V S/A cells, in which phosphorylation of the five most distal Ser is prevented by Ala substitution in the hDAT A559V background (Figure 5a, top).

Pretreatment of hDAT A559V S/A cells with the PKCβ-inhibitor does not significantly alter DA efflux (Figure 5a, bottom, compare striped bars ± PKCβ inhibitor). These data support a mechanism in which hDAT A559V must be phosphorylated at the N terminus to produce its ADE activity.

Next, we used the PKC inhibitor bisindolylmaleimide-I (BIM I) to probe changes in AMPH-induced DA efflux in hDAT A559V cells. In this experiment, we treated hDAT A559V cells either with BIM I (1 μM) or vehicle and then stimulated DA efflux with AMPH. BIM I restored the ability of AMPH to cause DA efflux in hDAT A559V cells (BIM I 0.20 ± 0.04 pA; $n = 3$; $P < 0.05$ by Student's *t*-test with respect to vehicle control). Furthermore, 1 μM of bisindolylmaleimide-V (BIM V, an inactive analog of BIM I) does not restore DA efflux in hDAT A559V cells ($P > 0.05$, Student's *t*-test, $n = 3$). Finally, to confirm the role of the PKCβII isoform specifically in maintaining ADE, we used a PKCβII inhibitor peptide (N-Myr-SLNPEWNET). Because the PKCβII peptide inhibitor is not cell permeable, we combined the whole-cell patch clamp technique with amperometry to allow perfusion of the PKCβII peptide inhibitor or scramble peptide into the cytoplasm with the whole-cell pipette. hDAT or hDAT A559V cells were whole-cell voltage clamped and loaded with 2 mM DA plus either the PKCβII inhibitor peptide (10 μM) or the scramble peptide (10 μM) for 10 min. The patch pipette was then lifted off the cell and AMPH-induced DA efflux was measured by an amperometric electrode juxtaposed to the intact, nonclamped cell. Amperometric current traces in response to 10 μM AMPH are displayed in Figure 5b (top). In hDAT cells, AMPH-induced DA efflux is not significantly different in cells perfused intracellularly with the PKCβII inhibitor peptide compared with the scramble peptide. Figure 5b bottom shows quantification of different experiments (compare filled bars ± PKCβ inhibitor). In contrast, the PKCβII inhibitor peptide restored AMPH-induced DA efflux in hDAT A559V cells, whereas the scramble peptide did not (Figure 5b, top). Quantification of multiple experiments is shown below the traces (compared open bars ± PKCβ inhibitor).

DISCUSSION

DAT has a critical role in regulating the strength and duration of dopaminergic neurotransmission by the clearing of extracellular DA. The capacity of DA clearance is finely dictated both by the number of active transporters at the plasma membrane and their turnover rate. In this study, we report aberrant functional phenotypes of hDAT A559V as compared with hDAT, possibly underlying disrupted DA neurotransmission and reward, two emerging hallmarks of ASD.[18,19,32,79–86] Although the A559V variant is not frequent enough to establish definitive causation for the complex disorder ASD, the striking functional phenotype suggests potential mechanisms contributing to complications in ASD. These may be convergent mechanisms reached through other means (that is, other DAT variants or variation in other genes related to dopaminergic neurotransmission) in ASD individuals who do not harbor the A559V variant. hDAT residue 559 is located within transmembrane domain 12 (TM12) near the extracellular side of the membrane (Supplementary Figure 3A). The recently published crystal structure of *Drosophila* DAT uncovered two surprising features near this region of the protein.[87] TM12 exhibits an unexpected kink away from the hydrophobic core of the transporter and following TM12 is a latch-like carboxy-terminal helix that caps the cytoplasmic gate. The impact of A559V Ala to Val substitution on DAT structure is unknown. However, it is intriguing to speculate that substitution of A559 with the bulkier Val side chain may increase the occurrence of steric clashes within TM12 (Supplementary Figures 3A and B). Such clashes could limit the structural flexibility of TM12 and potentially impact the conformational dynamics of hDAT including those involved in substrate translocation.

Using multiple techniques we found that hDAT A559V has reduced ability to transport AMPH, suggesting that conformational dynamics of the transporter are altered in the A559V variant. We hypothesized that the AMPH uptake impairment for hDAT A559V may confer its resistance to AMPH-induced DAT trafficking. Consistent with this hypothesis, bypassing the DAT requirement for cytosolic accumulation of AMPH via direct intracellular application of AMPH with a whole-cell electrode causes hDAT A559V cell surface redistribution. This is intriguing as hDAT A559V has normal transport of the substrate DA[1,34,45] and may suggest that differences exist between hDAT and hDAT A559V in terms of their ability to interact with AMPH.

We also found that PKCβ activity is constitutively elevated in hDAT A559V cells and that pharmacological inhibition of PKCβ restores AMPH transport as well as AMPH-induced DA efflux in these cells. Among other pathways D2Rs signaling stimulates PKCβ.[66] Intriguingly, it has previously been demonstrated that hDAT A559V cells have elevated D2R signaling.[1] Indeed, the D2R blocker raclopride inhibits ADE in neurons expressing hDAT A559V.[1] Therefore, it is intriguing to speculate that elevated PKCβ activity in hDAT A559V cells may stem from increased D2R signaling. It is important to note that ADE is inhibited by AMPH and that AMPH fails to cause DA efflux in hDAT A559V cells.[1,39] Here, we demonstrate that these anomalous AMPH actions in hDAT A559V cells are supported by elevated PKCβ activity. Inhibition of PKCβ restores the ability of AMPH to cause DA efflux.

The N terminus of DAT is a structural region for which phosphorylation at one or more of the five most distal Ser dictates reverse transport of DA.[88] Here, we demonstrated that these Ser (a possible target of PKCβ) are involved in this impaired ability of AMPH to cause DA efflux. Of note, hDAT A559V has higher levels of N terminus phosphorylation and that this phosphorylation contributes to DA efflux.[89] Mutating these five N-terminal Ser to Ala in the hDAT A559V background inhibits ADE and restores AMPH transport and the ability of AMPH to cause DA efflux. Substitution of these same Ser in the wild-type background of hDAT inhibits DA efflux,[88] highlighting a fundamental difference with regard to AMPH action in the A559V background, beyond the role of phosphorylation of the N terminus. Consistently, inhibition of PKCβ with three different pharmacological means, also restores the ability of AMPH to cause DA efflux. Collectively, these data suggest that phosphorylation of the hDAT A559V N terminus, through a PKCβ-dependent mechanism, regulates hDAT A559V conformation and the functional interaction with the DAT substrate AMPH, events of fundamental importance for AMPH to cause DA efflux.

In addition to exhibiting impaired AMPH-induced DA efflux, hDAT A559V also fails to traffic in response to AMPH. We demonstrate that the altered AMPH trafficking phenotype of hDAT A559V is conferred by constitutively elevated PKCβ activity. We show that PKCβ inhibition rescues the ability of AMPH to induce hDAT A559V trafficking. Notably, both hDAT[32] and PKCβ[90,91] dysfunction have been associated with ASD. The mechanism by which PKCβ inhibits hDAT A559V trafficking is unknown. However, our data suggest that it may involve DAT N-terminal phosphorylation. Consistent with this hypothesis, mutation of the most distal N terminus Ser to Ala rescues AMPH-induced DAT trafficking. These data provide a mechanistic framework where increased DAT N-terminal phosphorylation promoted by various signaling pathways, including D2R signaling through PKCβ, may underlie DA dysfunction in ASD.

Although the hDAT A559V variant is rare, the findings here provide valuable insights into the mechanisms of how dysregulated DA neurotransmission may represent a complication of ASD. These insights could shed light on the molecular mechanisms underlying the co-occurrence of ASD and ADHD, as this variant was previously found in two brothers with ADHD.[34,39] In all four subjects with known inheritance, A559V was transmitted from an

unaffected mother to a boy with a neurodevelopmental disorder, raising the possibility of a sex effect on penetrance. In this context, it also is important to note that co-occurring ADHD symptoms are common in ASD, reported in a large minority or even a majority of cases;[92–96] although neither of the subjects reported here had an existing diagnosis of ADHD. The frequent co-occurence of ADHD and ASD suggest dysregulation of common pathways across these two neurodevelopmental disorders, with our data suggesting DAT regulation as one such potential pathway. Therefore pharmacological approaches to compensating for imbalances in DA neurotransmission by targeting DAT may have potential therapeutic utility for some individuals with ASD, ADHD or combined ASD/ADHD. Notably, another DAT variant (R615C), that also results in altered DAT trafficking, was identified in an individual with ADHD.[97] Rare DAT variants have been observed in a range of disease populations and may confer risk for multiple complex psychiatric disorders through mechanisms that are as of yet unknown and warrant future investigation.

CONFLICT OF INTEREST

The authors declare no conflict of interest.

ACKNOWLEDGMENTS

This work was supported by NIH MH095044 (RDB), DA035263 (AG), DA012408 (AG), MH094400 (HC).

REFERENCES

1 Bowton E, Saunders C, Erreger K, Sakrikar D, Matthies HJ, Sen N *et al.* Dysregulation of dopamine transporters via dopamine D2 autoreceptors triggers anomalous dopamine efflux associated with attention-deficit hyperactivity disorder. *J Neurosci* 2010; **30**: 6048–6057.
2 Devlin B, Scherer SW. Genetic architecture in autism spectrum disorder. *Curr Opin Genet Dev* 2012; **22**: 229–237.
3 Sanders SJ, Murtha MT, Gupta AR, Murdoch JD, Raubeson MJ, Willsey AJ *et al.* De novo mutations revealed by whole-exome sequencing are strongly associated with autism. *Nature* 2012; **485**: 237–241.
4 Sanders Stephan J, Ercan-Sencicek AG, Hus V, Luo R, Murtha Michael T, Moreno-De-Luca D *et al.* Multiple recurrent de novo CNVs, including duplications of the 7q11.23 Williams Syndrome Region, are strongly associated with autism. *Neuron* 2011; **70**: 863–885.
5 Sebat J, Lakshmi B, Malhotra D, Troge J, Lese-Martin C, Walsh T *et al.* Strong association of de novo copy number mutations with autism. *Science* 2007; **316**: 445–449.
6 Pinto D, Pagnamenta AT, Klei L, Anney R, Merico D, Regan R *et al.* Functional impact of global rare copy number variation in autism spectrum disorders. *Nature* 2010; **466**: 368–372.
7 Levy D, Ronemus M, Yamrom B, Lee Y-h, Leotta A, Kendall J *et al.* Rare de novo and transmitted copy-number variation in autistic spectrum disorders. *Neuron* 2011; **70**: 886–897.
8 Cook EH Jr, Scherer SW. Copy-number variations associated with neuropsychiatric conditions. *Nature* 2008; **455**: 919–923.
9 Neale BM, Kou Y, Liu L, Ma'ayan A, Samocha KE, Sabo A *et al.* Patterns and rates of exonic de novo mutations in autism spectrum disorders. *Nature* 2012; **485**: 242–245.
10 O'Roak BJ, Vives L, Girirajan S, Karakoc E, Krumm N, Coe BP *et al.* Sporadic autism exomes reveal a highly interconnected protein network of de novo mutations. *Nature* 2012; **485**: 246–250.
11 Iossifov I, Ronemus M, Levy D, Wang Z, Hakker I, Rosenbaum J *et al.* De novo gene disruptions in children on the autistic spectrum. *Neuron* 2012; **74**: 285–299.
12 Cook EH Jr, Scherer SW. Copy-number variations associated with neuropsychiatric conditions. *Nature* 2008; **455**: 919–923.
13 Marshall CR, Noor A, Vincent JB, Lionel AC, Feuk L, Skaug J *et al.* Structural variation of chromosomes in autism spectrum disorder. *Am J Hum Genet* 2008; **82**: 477–488.
14 Weiss LA, Shen Y, Korn JM, Arking DE, Miller DT, Fossdal R *et al.* Association between microdeletion and microduplication at 16p11.2 and autism. *N Engl J Med* 2008; **358**: 667–675.
15 Björklund A, Dunnett SB. Fifty years of dopamine research. *Trends Neurosci* 2007; **30**: 185–187.
16 Giros B, Caron MG. Molecular characterization of the dopamine transporter. *Trends Pharmacol Sci* 1993; **14**: 43–49.
17 Palmiter RD. Dopamine signaling in the dorsal striatum is essential for motivated behaviors: lessons from dopamine-deficient mice. *Ann N Y Acad Sci* 2008; **1129**: 35–46.
18 Gadow KD, Roohi J, DeVincent CJ, Hatchwell E. Association of ADHD, tics, and anxiety with dopamine transporter (DAT1) genotype in autism spectrum disorder. *J Child Psychol Psychiatry* 2008; **49**: 1331–1338.
19 Nakamura K, Sekine Y, Ouchi Y, Tsujii M, Yoshikawa E, Futatsubashi M *et al.* Brain serotonin and dopamine transporter bindings in adults with high-functioning autism. *Arch Gen Psychiatry* 2010; **67**: 59–68.
20 Nguyen M, Roth A, Kyzar EJ, Poudel MK, Wong K, Stewart AM *et al.* Decoding the contribution of dopaminergic genes and pathways to autism spectrum disorder (ASD). *Neurochem Int* 2014; **66**: 15–26.
21 Farook MF, DeCuypere M, Hyland K, Takumi T, LeDoux MS, Reiter LT *et al.* Altered serotonin, dopamine and norepinepherine levels in 15q duplication and Angelman syndrome mouse models. *PLoS One* 2012; **7**: e43030.
22 Murray ML, Hsia Y, Glaser K, Simonoff E, Murphy DG, Asherson PJ *et al.* Pharmacological treatments prescribed to people with autism spectrum disorder (ASD) in primary health care. *Psychopharmacology* 2014; **231**: 1011–1021.
23 Dichter GS, Richey JA, Rittenberg AM, Sabatino A, Bodfish JW. Reward circuitry function in autism during face anticipation and outcomes. *J Autism Dev Disord* 2012; **42**: 147–160.
24 Scott-Van Zeeland AA, Dapretto M, Ghahremani DG, Poldrack RA, Bookheimer SY. Reward processing in autism. *Autism Res* 2010; **3**: 53–67.
25 Abrams DA, Lynch CJ, Cheng KM, Phillips J, Supekar K, Ryali S *et al.* Underconnectivity between voice-selective cortex and reward circuitry in children with autism. *Proc Natl Acad Sci USA* 2013; **110**: 12060–12065.
26 Gordon EM, Stollstorff M, Devaney JM, Bean S, Vaidya CJ. Effect of dopamine transporter genotype on intrinsic functional connectivity depends on cognitive state. *Cereb Cortex* 2012; **22**: 2182–2196.
27 Tureck K, Matson JL, Cervantes P, Turygin N. Autism severity as a predictor of inattention and impulsivity in toddlers. *Dev Neurorehabil* 2013; doi: 10.3109/17518423.2013.807884; e-pub ahead of print.
28 Kristensen AS, Andersen J, Jorgensen TN, Sorensen L, Eriksen J, Loland CJ *et al.* SLC6 neurotransmitter transporters: structure, function, and regulation. *Pharmacol Rev* 2011; **63**: 585–640.
29 Giros B, Jaber M, Jones SR, Wightman RM, Caron MG. Hyperlocomotion and indifference to cocaine and amphetamine in mice lacking the dopamine transporter. *Nature* 1996; **379**: 606–612.
30 Volkow ND, Chang L, Wang GJ, Fowler JS, Franceschi D, Sedler M *et al.* Loss of dopamine transporters in methamphetamine abusers recovers with protracted abstinence. *J Neurosci* 2001; **21**: 9414–9418.
31 Volkow ND, Wang GJ, Fischman MW, Foltin RW, Fowler JS, Abumrad NN *et al.* Relationship between subjective effects of cocaine and dopamine transporter occupancy. *Nature* 1997; **386**: 827–830.
32 Hamilton PJ, Campbell NG, Sharma S, Erreger K, Herborg Hansen F, Saunders C *et al.* De novo mutation in the dopamine transporter gene associates dopamine dysfunction with autism spectrum disorder. *Mol Psychiatry* 2013; **18**: 1315–1323.
33 Mazei-Robison MS, Couch RS, Shelton RC, Stein MA, Blakely RD. Sequence variation in the human dopamine transporter gene in children with attention deficit hyperactivity disorder. *Neuropharmacology* 2005; **49**: 724–736.
34 Mazei-Robison MS, Blakely RD. Expression studies of naturally occurring human dopamine transporter variants identifies a novel state of transporter inactivation associated with Val382Ala. *Neuropharmacology* 2005; **49**: 737–749.
35 Dreher JC, Kohn P, Kolachana B, Weinberger DR, Berman KF. Variation in dopamine genes influences responsivity of the human reward system. *Proc Natl Acad Sci USA* 2009; **106**: 617–622.
36 Hoogman M, Onnink M, Cools R, Aarts E, Kan C, Vasquez AA *et al.* The dopamine transporter haplotype and reward-related striatal responses in adult ADHD. *Eur Neuropsychopharmacol* 2013; **23**: 469–478.
37 Enter D, Colzato LS, Roelofs K. Dopamine transporter polymorphisms affect social approach-avoidance tendencies. *Genes Brain Behav* 2012; **11**: 671–676.
38 Grunhage F, Schulze TG, Muller DJ, Lanczik M, Franzek E, Albus M *et al.* Systematic screening for DNA sequence variation in the coding region of the human dopamine transporter gene (DAT1). *Mol Psychiatry* 2000; **5**: 275–282.
39 Mazei-Robison MS, Bowton E, Holy M, Schmudermaier M, Freissmuth M, Sitte HH *et al.* Anomalous dopamine release associated with a human dopamine transporter coding variant. *J Neurosci* 2008; **28**: 7040–7046.
40 Liu J, Nyholt DR, Magnussen P, Parano E, Pavone P, Geschwind D *et al.* A genomewide screen for autism susceptibility loci. *Am J Hum Genet* 2001; **69**: 327–340.
41 Lord C, Rutter M, Le Couteur A. Autism Diagnostic Interview-Revised: a revised version of a diagnostic interview for caregivers of individuals with possible pervasive developmental disorders. *J Autism Dev Disord* 1994; **24**: 659–685.

42 Lord C, Risi S, Lambrecht L, Cook EH Jr, Leventhal BL, DiLavore PC *et al.* The autism diagnostic observation schedule-generic: a standard measure of social and communication deficits associated with the spectrum of autism. *J Autism Dev Disord* 2000; **30**: 205–223.
43 Lim ET, Raychaudhuri S, Sanders SJ, Stevens C, Sabo A, MacArthur DG *et al.* Rare complete knockouts in humans: population distribution and significant role in autism spectrum disorders. *Neuron* 2013; **77**: 235–242.
44 Liu L, Sabo A, Neale BM, Nagaswamy U, Stevens C, Lim E *et al.* Analysis of rare, exonic variation amongst subjects with autism spectrum disorders and population controls. *PLoS Genet* 2013; **9**: e1003443.
45 Mazei-Robison MSB, Bowton E, Holy M, Schmudermaier M, Freissmuth M, Sitte HH *et al.* Anomalous dopamine release associated with a human dopamine transporter coding variant. *J Neurosci* 2008; **28**: 7040–7046.
46 Sung U, Apparsundaram S, Galli A, Kahlig KM, Savchenko V, Schroeter S *et al.* A regulated interaction of syntaxin 1A with the antidepressant-sensitive norepinephrine transporter establishes catecholamine clearance capacity. *J Neurosci* 2003; **23**: 1697–1709.
47 Garcia BG, Wei Y, Moron JA, Lin RZ, Javitch JA, Galli A *et al.* Akt is essential for insulin modulation of amphetamine-induced human dopamine transporter cell-surface redistribution. *Mol Pharmacol* 2005; **68**: 102–109.
48 Wei Y, Williams JM, Dipace C, Sung U, Javitch JA, Galli A *et al.* Dopamine transporter activity mediates amphetamine-induced inhibition of Akt through a Ca2 +/calmodulin-dependent kinase II-dependent mechanism. *Mol Pharmacol* 2007; **71**: 835–842.
49 Saunders C, Ferrer JV, Shi L, Chen J, Merrill G, Lamb ME *et al.* Amphetamine-induced loss of human dopamine transporter activity: an internalization-dependent and cocaine-sensitive mechanism. *Proc Natl Acad Sci USA* 2000; **97**: 6850–6855.
50 Takahashi H, Suzuki K, Namiki H. Phenylarsine oxide and H2O2 plus vanadate induce reverse translocation of phorbol-ester-activated PKCbetaII. *Cell Struct Funct* 2003; **28**: 123–130.
51 Mager S, Naeve J, Quick M, Labarca C, Davidson N, Lester HA *et al.* Steady states, charge movements, and rates for a cloned GABA transporter expressed in Xenopus oocytes. *Neuron* 1993; **10**: 177–188.
52 Zhu SJ, Kavanaugh MP, Sonders MS, Amara SG, Zahniser NR. Activation of protein kinase C inhibits uptake, currents and binding associated with the human dopamine transporter expressed in Xenopus oocytes. *J Pharmacol Exp Ther* 1997; **282**: 1358–1365.
53 Kahlig KM, Javitch JA, Galli A. Amphetamine regulation of dopamine transport. Combined measurements of transporter currents and transporter imaging support the endocytosis of an active carrier. *J Biol Chem* 2004; **279**: 8966–8975.
54 Lute BJ, Khoshbouei H, Saunders C, Sen N, Lin RZ, Javitch JA *et al.* PI3K signaling supports amphetamine-induced dopamine efflux. *Biochem Biophys Res Commun* 2008; **372**: 656–661.
55 Cremona ML, Matthies HJ, Pau K, Bowton E, Speed N, Lute BJ *et al.* Flotillin-1 is essential for PKC-triggered endocytosis and membrane microdomain localization of DAT. *Nat Neurosci* 2011; **14**: 469–477.
56 Robertson SD, Matthies HJ, Galli A. A closer look at amphetamine-induced reverse transport and trafficking of the dopamine and norepinephrine transporters. *Mol Neurobiol* 2009; **39**: 73–80.
57 Boudanova E, Navaroli DM, Melikian HE. Amphetamine-induced decreases in dopamine transporter surface expression are protein kinase C-independent. *Neuropharmacology* 2008; **54**: 605–612.
58 Johnson LA, Furman CA, Zhang M, Guptaroy B, Gnegy ME. Rapid delivery of the dopamine transporter to the plasmalemmal membrane upon amphetamine stimulation. *Neuropharmacology* 2005; **49**: 750–758.
59 Gulley JM, Doolen S, Zahniser NR. Brief, repeated exposure to substrates down-regulates dopamine transporter function in Xenopus oocytes in vitro and rat dorsal striatum in vivo. *J Neurochem* 2002; **83**: 400–411.
60 Sulzer D, Sonders MS, Poulsen NW, Galli A. Mechanisms of neurotransmitter release by amphetamines: a review. *Prog Neurobiol* 2005; **75**: 406–433.
61 Kahlig KM, Lute BJ, Wei Y, Loland CJ, Gether U, Javitch JA *et al.* Regulation of dopamine transporter trafficking by intracellular amphetamine. *Mol Pharmacol* 2006; **70**: 542–548.
62 Mahajan R, Bernal MP, Panzer R, Whitaker A, Roberts W, Handen B *et al.* Clinical practice pathways for evaluation and medication choice for attention-deficit/hyperactivity disorder symptoms in autism spectrum disorders. *Pediatrics* 2012; **130**: S125–S138.
63 Cortese S, Castelnau P, Morcillo C, Roux S, Bonnet-Brilhault F. Psychostimulants for ADHD-like symptoms in individuals with autism spectrum disorders. *Expert Rev Neurother* 2012; **12**: 461–473.
64 Zaczek R, Culp S, De Souza EB. Interactions of [3H]amphetamine with rat brain synaptosomes. II. Active transport. *J Pharmacol Exp Ther* 1991; **257**: 830–835.
65 Erreger KG, Grewer C, Javitch J, Galli A. Currents in response to rapid concentration jumps of amphetamine uncover novel aspects of human dopamine transporter function. *J Neurosci* 2008; **28**: 976–989.
66 Chen R, Daining CP, Sun H, Fraser R, Stokes SL, Leitges M *et al.* Protein kinase Cbeta is a modulator of the dopamine D2 autoreceptor-activated trafficking of the dopamine transporter. *J Neurochem* 2013; **125**: 663–672.
67 Loder MK, Melikian HE. The dopamine transporter constitutively internalizes and recycles in a protein kinase C-regulated manner in stably transfected PC12 cell lines. *J Biol Chem* 2003; **278**: 22168–22174.
68 Holton KL, Loder MK, Melikian HE. Nonclassical, distinct endocytic signals dictate constitutive and PKC-regulated neurotransmitter transporter internalization. *Nat Neurosci* 2005; **8**: 881–888.
69 Sorkina T, Hoover BR, Zahniser NR, Sorkin A. Constitutive and protein kinase C-induced internalization of the dopamine transporter is mediated by a clathrin-dependent mechanism. *Traffic* 2005; **6**: 157–170.
70 Owens WA, Williams JM, Saunders C, Avison MJ, Galli A, Daws LC *et al.* Rescue of dopamine transporter function in hypoinsulinemic rats by a D2 receptor-ERK-dependent mechanism. *J Neurosci* 2012; **32**: 2637–2647.
71 Speed N, Saunders C, Davis A, Owens W, Matthies H, Saadat S *et al.* Impaired Striatal Akt Signaling Disrupts Dopamine Homeostasis and Increases Feeding. *PLoS One* 2011; **6**: 1–10.
72 Speed NK, Matthies HJ, Kennedy JP, Vaughan RA, Javitch JA, Russo SJ *et al.* Akt-dependent and isoform-specific regulation of dopamine transporter cell surface expression. *ACS Chem Neurosci* 2010; **1**: 476–481.
73 Williams JM, Owens WA, Turner GH, Saunders C, Dipace C, Blakely RD *et al.* Hypoinsulinemia regulates amphetamine-induced reverse transport of dopamine. *PLoS Biol* 2007; **5**: 2369–2378.
74 Johnson LA, Guptaroy B, Lund D, Shamban S, Gnegy ME. Regulation of amphetamine-stimulated dopamine efflux by protein kinase C beta. *J Biol Chem* 2005; **280**: 10914–10919.
75 Newton AC. Protein kinase C: poised to signal. *Am J Physiol Endocrinol Metab* 2010; **298**: E395–E402.
76 Parekh DB, Ziegler W, Parker PJ. Multiple pathways control protein kinase C phosphorylation. *EMBO J* 2000; **19**: 496–503.
77 Steinberg SF. Structural basis of protein kinase C isoform function. *Physiol Rev* 2008; **88**: 1341–1378.
78 Ron D, Luo JH, Mochlyrosen D. C2 region-derived peptides inhibit translocation and function of beta-protein kinase-c in-vivo. *J Biol Chem* 1995; **270**: 24180–24187.
79 Anderson BM, Schnetz-Boutaud N, Bartlett J, Wright HH, Abramson RK, Cuccaro ML *et al.* Examination of association to autism of common genetic variationin genes related to dopamine. *Autism Res* 2008; **1**: 364–369.
80 Hettinger JA, Liu X, Schwartz CE, Michaelis RC, Holden JJ. A DRD1 haplotype is associated with risk for autism spectrum disorders in male-only affected sib-pair families. *Am J Med Genet B Neuropsychiatr Genet* 2008; **147B**: 628–636.
81 Staal WG, de Krom M, de Jonge MV. Brief report: the dopamine-3-receptor gene (DRD3) is associated with specific repetitive behavior in autism spectrum disorder (ASD). *J Autism Dev Disord* 2012; **42**: 885–888.
82 Nieminen-von Wendt TS, Metsahonkala L, Kulomaki TA, Aalto S, Autti TH, Vanhala R *et al.* Increased presynaptic dopamine function in Asperger syndrome. *Neuroreport* 2004; **15**: 757–760.
83 Gadow KD, DeVincent CJ, Olvet DM, Pisarevskaya V, Hatchwell E. Association of DRD4 polymorphism with severity of oppositional defiant disorder, separation anxiety disorder and repetitive behaviors in children with autism spectrum disorder. *Eur J Neurosci* 2010; **32**: 1058–1065.
84 de Krom M, Staal WG, Ophoff RA, Hendriks J, Buitelaar J, Franke B *et al.* A common variant in DRD3 receptor is associated with autism spectrum disorder. *Biol Psychiatry* 2009; **65**: 625–630.
85 Makkonen I, Kokki H, Kuikka J, Turpeinen U, Riikonen R. Effects of fluoxetine treatment on striatal dopamine transporter binding and cerebrospinal fluid insulin-like growth factor-1 in children with autism. *Neuropediatrics* 2011; **42**: 207–209.
86 Dolen G, Darvishzadeh A, Huang KW, Malenka RC. Social reward requires coordinated activity of nucleus accumbens oxytocin and serotonin. *Nature* 2013; **501**: 179–184.
87 Penmatsa A, Wang KH, Gouaux E. X-ray structure of dopamine transporter elucidates antidepressant mechanism. *Nature* 2013; **503**: 85–90.
88 Khoshbouei H, Sen N, Guptaroy B, Johnson L, Lund D, Gnegy ME *et al.* N-terminal phosphorylation of the dopamine transporter is required for amphetamine-induced efflux. *PLoS Biol* 2004; **2**: E78.
89 Kahlig KM, Binda F, Khoshbouei H, Blakely RD, McMahon DG, Javitch JA *et al.* Amphetamine induces dopamine efflux through a dopamine transporter channel. *Proc Natl Acad Sci USA* 2005; **102**: 3495–3500.

90 Philippi A, Roschmann E, Tores F, Lindenbaum P, Benajou A, Germain-Leclerc L *et al.* Haplotypes in the gene encoding protein kinase c-beta (PRKCB1) on chromosome 16 are associated with autism. *Mol Psychiatry* 2005; **10**: 950–960.
91 Lintas C, Sacco R, Garbett K, Mirnics K, Militerni R, Bravaccio C *et al.* Involvement of the PRKCB1 gene in autistic disorder: significant genetic association and reduced neocortical gene expression. *Mol Psychiatry* 2009; **14**: 705–718.
92 Matson JL, Rieske RD, Williams LW. The relationship between autism spectrum disorders and attention-deficit/hyperactivity disorder: an overview. *Res Dev Disabil* 2013; **34**: 2475–2484.
93 Goldstein S, Schwebach AJ. The comorbidity of pervasive developmental disorder and attention deficit hyperactivity disorder: results of a retrospective chart review. *J Autism Dev Disord* 2004; **34**: 329–339.
94 Yoshida Y, Uchiyama T. The clinical necessity for assessing Attention Deficit/Hyperactivity Disorder (AD/HD) symptoms in children with high-functioning Pervasive Developmental Disorder (PDD). *Eur Child Adolesc Psychiatry* 2004; **13**: 307–314.
95 Gadow KD, DeVincent CJ, Schneider J. Comparative study of children with ADHD only, autism spectrum disorder plus ADHD, and chronic multiple tic disorder plus ADHD. *J Atten Disord* 2009; **12**: 474–485.
96 Rao PA, Landa RJ. Association between severity of behavioral phenotype and comorbid attention deficit hyperactivity disorder symptoms in children with autism spectrum disorders. *Autism* 2014; **18**: 272–280.
97 Sakrikar D, Mazei-Robison MS, Mergy MA, Richtand NW, Han Q, Hamilton PJ *et al.* Attention deficit/hyperactivity disorder-derived coding variation in the dopamine transporter disrupts microdomain targeting and trafficking regulation. *J Neurosci* 2012; **32**: 5385–5397.

Supplementary Information accompanies the paper on the Translational Psychiatry website (http://www.nature.com/tp)